Quaternary Structure Built from Subunits Combining NMR and Small-Angle X-Ray Scattering Data

Maija-Liisa Mattinen,* Kimmo Pääkkönen,* Teemu Ikonen,† Jeremy Craven,‡ Torbjörn Drakenberg,* Ritva Serimaa,† Jonathan Waltho,‡ and Arto Annila†

*VTT Biotechnology, FIN-02044 VTT, Espoo, Finland; †Department of Physical Sciences, University of Helsinki, FIN-00014 Helsinki, Finland; and ‡Department of Molecular Biology and Biotechnology, University of Sheffield, Sheffield S10 2TN, United Kingdom

ABSTRACT A new principle in constructing molecular complexes from the known high-resolution domain structures joining data from NMR and small-angle x-ray scattering (SAXS) measurements is described. Structure of calmodulin in complex with trifluoperazine was built from N- and C-terminal domains oriented based on residual dipolar couplings measured by NMR in a dilute liquid crystal, and the overall shape of the complex was derived from SAXS data. The residual dipolar coupling data serves to reduce angular degrees of freedom, and the small-angle scattering data serves to confine the translational degrees of freedom. The complex built by this method was found to be consistent with the known crystal structure. The study demonstrates how approximate tertiary structures of modular proteins or quaternary structures composed of subunits can be assembled from high-resolution structures of domains or subunits using mutually complementary NMR and SAXS data.

INTRODUCTION

Spatial rearrangements between and within proteins during the course of biological function are essential manifestations of life at the molecular level. Large organizational and conformational changes often challenge the means currently available for the determination of three-dimensional structures. Crystals of a protein in all of its relevant conformations are seldom available, in particular when one or more states in the functional pathway exhibit flexibility. NMR-derived distance information for large complexes is sparse, especially between subunits. Here we show that a combination of directional information measured by NMR from weakly aligned systems (Tjandra and Bax, 1997; Bax et al., 2001) with global information about size and shape embedded in small-angle scattering (SAS) of x-rays or neutrons (Glatter and Kratky, 1982; Feigin and Svergun, 1987) greatly extends the ability to construct models of larger modular structures in solution based on high-resolution data.

Small-angle scattering of x-rays or neutrons is sensitive to the overall size and shape of a protein or its complex (Trewhella, 1997; Doniach, 2001). When employing neutrons (SANS), contrast can be created from the large difference in the scattering lengths of H and D by isotopic H/D exchange, perdeuteration of the subunits, and varying the deuterium oxide content of the solvent (Koch and Stuhrmann, 1979). On the basis of the scattered intensity, low-resolution envelopes can be constructed ab initio by various ways (Stuhrmann 1970; Chacon et al., 1998; Svergun, 1999). However, provided that the subunit structures of a quaternary complex are known to high resolution, the arrangement of the subunits can be searched by finding the best fit between the experimental scattered intensity $I(s)$ and amplitudes computed from two-body structures according to

$$I(\mathbf{s}) = \langle |A_a(\mathbf{s}) - \rho_s A_s(\mathbf{s}) + \delta\rho_b A_b(\mathbf{s})|^2 \rangle_\Omega \qquad (1)$$

where $\mathbf{s}$ is the scattering vector of the incident photons, $A_a(\mathbf{s})$, $A_s(\mathbf{s})$, and $A_b(\mathbf{s})$ are the scattering amplitudes from the particle in vacuum, the volume excluded by the particle, and the hydration shell, respectively, ρ_s is the electron density of the solvent and $\delta\rho_b$ is the contrast of the hydration shell (Svergun et al., 1995). Only the cross-term that arises from the two-particle interference needs to be computed at each node. The computational load of the grid that comprises N^3 translational and M^3 rotational nodes is nevertheless formidable to explore the space in detail. Here N refers to the number of points along each Cartesian axis and M to the number of points along the three angular variables. The radial separation between the subunits can often be obtained to a high precision. However, the rotational degrees of freedom, i.e., how to orient the domains relative to each other, remain ambiguous. Only a few proteins are sufficiently asymmetric to give $I(s)$ with sufficient detail to resolve this ambiguity, which also requires that the intensity is measured with a large enough statistical precision to enable the use of its high-angle part (Müller et al., 1990; Svergun et al., 2001).

The rotational uncertainty remaining from SAS measurements could be resolved using NMR. Enhanced anisotropic tumbling of molecules in a liquid crystal (Tjandra and Bax, 1997; Hansen et al., 1998) gives rise to readily observable

Submitted October 31, 2001, and accepted for publication February 19, 2002.

Address reprint requests to Dr. Arto Annila, Institute of Biotechnology, University of Helsinki, P.O. Box 56, FIN-00014 Helsinki, Finland. Tel.: 358-9-191-50629; Fax: 358-9-191-50639; E-mail: arto.annila@helsinki.fi.

0006-3495/02/08/1177/07 $2.00

residual dipolar couplings, $D(\theta, \phi)$, which depend on the polar coordinates θ and ϕ of the internuclear vector relative to the principal axes of the molecular alignment tensor **A**:

$$D(\theta, \phi) = A_{\parallel}\left[3\cos^2\theta - 1 + \frac{3}{2} R \sin^2\theta \cos 2\phi\right] \quad (2)$$

where $A_{\parallel}$ is the axial and $A_{\perp}$ is the transverse component of **A**; i.e., $R = A_{\perp}/A_{\parallel}$ is the rhombicity (Bastiaan et al., 1987; Clore et al., 1998; Losonczi et al., 1999). Residual dipolar couplings can also be measured from proteins with intrinsically high magnetic susceptibility (Tolman et al., 1997; Biekofsky et al., 1999), including protein-DNA complexes (Clore and Gronenborn 1998).

Main-chain dipolar couplings are the most attainable to measure and to assign (Ottiger et al., 1998; Permi and Annila 2000; Permi et al., 2000). Values of dipolar couplings relate the N-H bond directions to the principal axes system (PAS) of the molecular alignment tensor (**A**) (Eq. 3). The elements of the traceless and symmetric **A** in the molecular frame can be determined by singular value decomposition, using the measured dipolar couplings and projection angles of corresponding internuclear vectors derived from the known domain structures (Losonczi et al., 1999). The diagonalization of **A** makes the molecular and principal frames coincide and yields a rotation matrix $\mathbf{R} \in O_3^+$ that transforms the coordinates to the PAS.

The complex between calmodulin (CaM) and trifluoperazine (TFP) was chosen to illustrate the method and to assess the accuracy and precision that can be obtained. The CaM system is very well defined structurally and has already required a combination of structural methods for a correct molecular description of its function. The rigid connectivity between the N- and C-terminal domains observed in the crystal (Chattopadhyaya et al., 1992) was shown not to be retained in solution using small-angle x-ray scattering (Heidorn and Trewhella 1988; Heidorn et al., 1989) and NMR relaxation measurements (Barbato et al., 1992) and recently by means of residual dipolar couplings (Chou et al., 2001). The two domains are relatively extended and independently mobile. However, in the presence of models of the natural targets, NMR (Ikura et al., 1992a; Ikura et al., 1992b) and x-ray structures (Meador et al., 1992) have revealed that the two domains bind such peptides in a more compact, globular complex. Similarly, hydrophobic ligands can also shift the equilibrium position from independently mobile domains toward a compact globular structure (Vandonselaar et al., 1994; Cook et al., 1994; Osawa et al., 1998, 1999). According to x-ray scattering (SAXS) measurements, the CaM-TFP complex predominantly populates a compact globular form (Matsushima et al., 2000), in which more than five times molar excess of TFP is required to reach full occupancy. The positions of four TFP molecules have been defined by x-ray diffraction (1LIN) (Vandonselaar et al., 1994), two of which occupy higher-affinity sites (Matsushima et al., 2000; Craven et al., 1996).

MATERIALS AND METHODS

Calmodulin was produced and purified as described earlier (Craven et al., 1996). Samples for NMR measurements were 0.3 mM in dilute liquid crystals. Liquid crystal media for NMR measurements were prepared by dissolving to an approximate concentration of 30 mg ml^{-1} filamentous phage (Pf1) particles that align in the magnetic field (Hansen et al., 1998). The actual aligning power of the medium was quantified from the deuterium quadrupolar splitting of deuterium oxide. All spectra were recorded using Varian 800 and 600 NMR spectrometers.

For each residue of CaM the main-chain N-H heteronuclear splittings between multiplet components were measured from α/β half-filtered $^{15}N,^{1}H$ correlation spectra (Cordier et al., 1999) at 37°C in 18 h. The dipolar contribution to an N-H splitting was obtained by subtracting the scalar coupling measured from reference spectra recorded from 0.5 mM sample in water. The five independent elements of the traceless and symmetric molecular alignment tensor were determined by singular value decomposition.

The SAXS experiments were carried out with CuK_{α} radiation made monochromatic with a Ni filter and a totally reflecting mirror. Radiation was obtained from a sealed fine-focus x-ray tube and detected by a linear one-dimensional position-sensitive proportional counter (MBraun OED 50M). The beam has a narrow profile; together with detector resolution the instrumental function has FWHM = 0.005 $Å^{-1}$ horizontally and FWHM = 0.35 $Å^{-1}$ vertically. The sample was injected with a syringe in a steel-framed cell that has thin stretched polyimide foils as flat windows. The protein concentration was 0.3 mM. The measurements were made at room temperature using 3 h of accumulation time. The sample-to-detector distance was 165 mm. The background and non-sample scattering was measured separately and subtracted from each measurement. The scattered intensity was corrected for the instrumental broadening, and the distance distribution function was calculated using the program GNOM (Svergun 1992).

RESULTS

The complexation of CaM with TFP molecules causes a large change in $P(r)$ (Fig. 1), characterized by a reduction in the radius of gyration (R_g) from 20.3 to 17.9 Å and in the longest diameter D_{max} from ~65 to 55 Å. This is indicative of the transition to a compact globular form (Heidorn et al., 1989; Osawa et al., 1999).

Residual main chain ^{15}N-^{1}H dipolar couplings (D_{NH}) were measured in the presence of more than fivefold molar excess of TFP in a dilute liquid crystalline phase (Fig. 2). The principal frames of each CaM domain in the complex with TFP were determined independently, using the coordinates of free CaM (1CLL) rather than the TFP complex form (1LIN) to be consistent with the notion of building quaternary complexes from unligated subunits. Residues from the central helix in the vicinity of the mobile region, residues subject to rapid transverse relaxation, and data points with poor signal-to-noise ratio were not included. The calculated $D(\theta, \phi)$ values agree closely with the measured data (Fig. 2). The RMSD is 2.2 and 1.8 Hz for the N- and C-domains, respectively. The uncertainty in **A** was estimated on the basis of the variation in the diagonal elements of **A** introduced by a jackknife procedure (Shao and Tu, 1995), deleting on average 10% of the measured data points at random 20,000 times. This simulates the

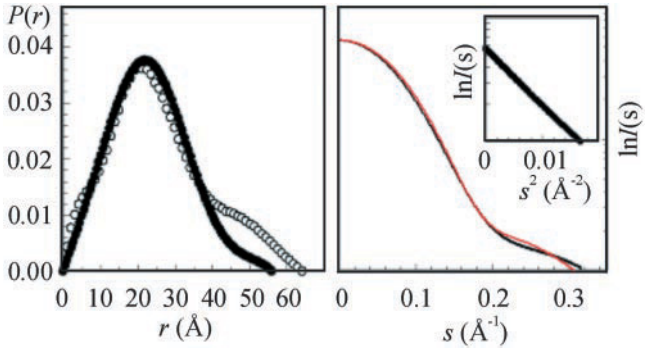

FIGURE 1 (*Left*) Distance distribution function $P(r)$ of free CaM (○) obtained from small-angle x-ray scattering measurements. The scattered intensity of x-rays from 4· Ca^{2+}-CaM is similar to that reported previously (Heidorn and Trewhella, 1988; Osawa et al., 1999) and corresponds to a mobile two-domain structure with a shorter interdomain distance than is expected on the basis of the crystal structure (1CLL, Chattopadhyaya et al., 1992). No single conformation exists that would give a SAXS intensity curve in a good agreement with the measured data. When trifluoperazine is added to the solution a structural change from an elongated and mobile conformation to a compact globular structure occurs that is observed as change in $P(r)$ (●). (*Right*) The scattered intensity $I(s)$ vs. $s = 4\pi\sin\theta/\lambda$ (*solid line*), where 2θ is the scattering angle and λ the wavelength, was compared with the computed from the model built on the basis of NMR and SAXS data (see text) (*red line*) shown in Fig. 4. The Guiner plot in the inset shows no sign of aggregation.

experimental situation where data points are lost due to poor signal-to-noise ratio or signal overlap. The half-widths and base widths of A_{xx}, A_{yy}, and A_{zz} distributions are ~0.5 Hz and 2.0 Hz, respectively, for both domains. This corresponds to the 1.2-Å RMSD and standard deviation of 2.6 Å (N-domain) and 1.6-Å RMSD and 1.3-Å SD (C-domain) between the 20,000 family members. The correlation between the measured and computed values of D_{NH} are r = 0.95–0.89 (N-domain) and r = 0.93–0.82 (C-domain). The uncertainties obtained above are similar in magnitude to those obtained from Monte-Carlo simulations using 1-Hz imprecision in the measurement of dipolar couplings. The quality factors (Ottiger and Bax, 1999) for the optimum orientations were 0.23 and 0.37 for the N- and C-domains, respectively. The PAS orientations of the individual domains closely coincide, as expected for a compact globular system. The correlation decreases marginally to 0.91 when the N- and C-domain data are fitted simultaneously. Therefore, changes in the dipolar couplings due to complex formation can primarily be attributed to changes in the relative orientation of the domains rather than to changes in domain structure.

Comparisons similar to those above using on the average 80% of the experimental values yielded families of domain orientations with RMSDs (SD) of 2.7 (4.9) and 2.5 (1.9) Å for the N- and C-domains, respectively, and with only 50% of the experimental values 6.0 (6.9) and 6.0 (5.2) Å for the N- and C-domains, respectively. Obviously, the smaller the number of residual dipolar couplings used in the determination the poorer the precision. Also, the choice of nonredundant directions becomes important as is reflected by the increasing deviation among orientations.

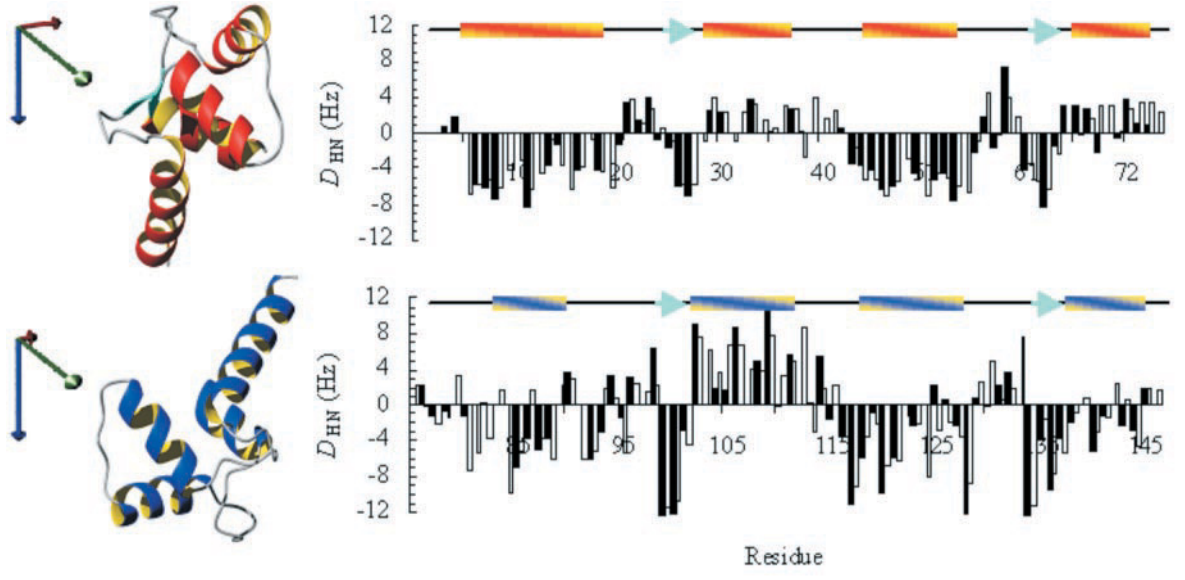

FIGURE 2 Main-chain N-H residual dipolar couplings (*closed bars*) along the amino acid sequence of calmodulin in the complex with trifluoperazine, measured from the N-terminal domain (above) and C-terminal domain (below). A dipolar coupling relates to the orientation of the corresponding N-H vector with respect to the molecular alignment tensor that were determined independently for each domain from 105 dipolar couplings excluding residues subject to rapid transverse relaxation and poor signal-to-noise ratio. The D_{NH} values (*open bars*) were computed from the domains of CaM (1CLL) in their alignment frames with axial components shown on left. The secondary structures, helices in yellow-red and β-sheets in cyan, are indicated for the N- and C-terminal domains.

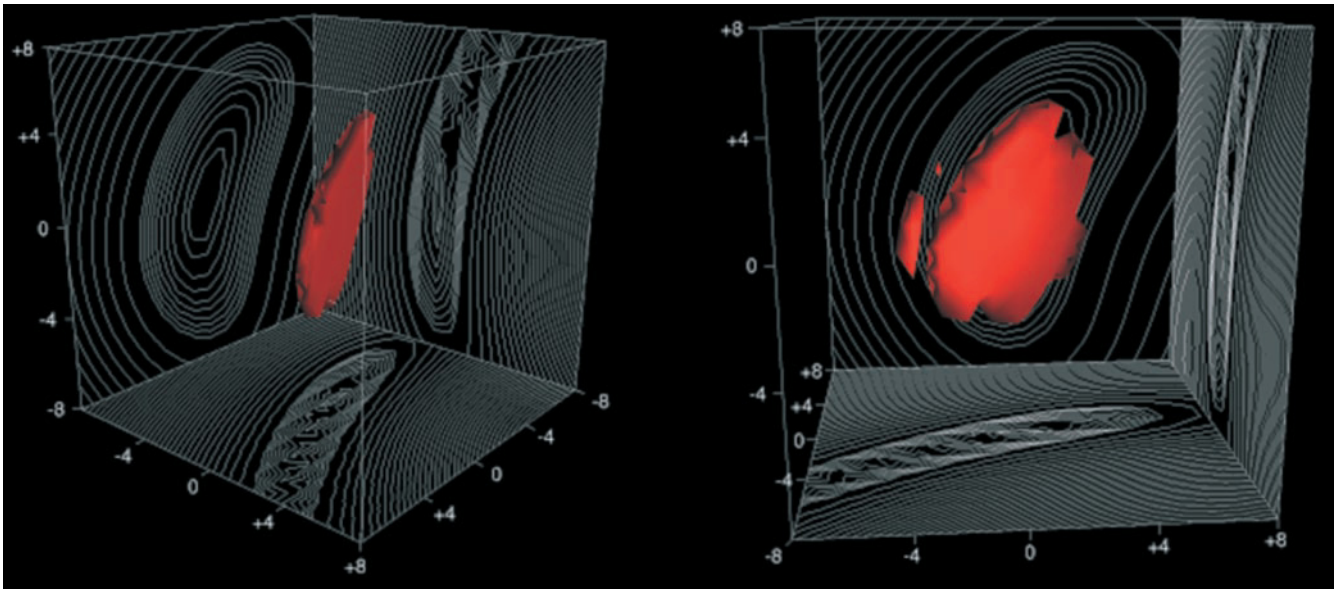

FIGURE 3 Spatial precision of the two-domain model of calmodulin-TFP complex with tangential (*left*) and radial (*right*) projections. The N-domain in its NMR-derived alignment frame was kept in a fixed position and the position of the C-domain in its alignment frame was searched by placing it at the Cartesian grid points separated by 1 Å and calculating least-squares fit to SAXS data. The grid point with the lowest χ^2 value is in the origin (*center*) of the figures. The red surfaces are drawn at a constant χ^2 with a value of minimum $\chi^2 = +3.5$, which corresponds to the uncertainty area of the three-parameter fit. The faces of the cubes show cuts of the data taken through the χ^2 minimum as contour plots.

Four possible relationships between the two domains of CaM result from the fitting procedure, because residual dipolar couplings are even functions of θ and ϕ (Eq. 3). In this particular case the comparatively short linker between the domains of CaM imposes a covalent constraint that excludes two of the four possibilities. The remaining two can be readily distinguished from the χ^2 value when the SAXS data are included. In general, the feasibility of this procedure for choosing the appropriate symmetry alternative depends on the overall shape of the complex and subunits, but the CaM domains are not unusually irregular in shape. Alternatively, the fourfold degeneracy can be lifted by recording data from the complex in another orientation utilizing a different liquid crystal (Al-Hashimi et al., 2000).

The relative position of the pre-oriented domains was determined from SAXS data by minimizing the sum of least-squares between the measured $I_{exp}(s)$ and computed $I(s)$, defined as

$$\chi^2 = \frac{1}{N-1}\sum_{j=1}^{N}\left[\frac{I(s_j) - I_{exp}(s_j)}{\sigma(s_j)}\right]^2, \qquad (3)$$

where $\sigma(s)$ is the standard deviation of the recorded scattering curve. The model intensity $I(s)$ was obtained from the atomic coordinates by the Debye formula. The coordinates of the model were transformed by changing the relative position of the domains according to a given translation vector. The minimum of χ^2 equal to 3.5 was sought as a function of the three interdomain distance parameters with the nonlinear optimization algorithm of Nelder and Mead. For the radius of gyration our model yielded $R_g = 17.7$ Å. A similar comparison between experimental and model $P(r)$ functions was also made yielding similar results.

The precision of the minimum position was considered by computing χ^2 in a grid with a 1-Å spacing around the minimum (Fig. 3). The distance between the domains is obtained with a good precision of ± 1 Å because the SAXS data are intrinsically highly sensitive to R_g. However, the perpendicular precision is more modest, ± 4 Å on a convex surface, equivalent to a nearly conical distribution of $\pm 10°$.

Although the Debye formula does not take into account such important factors as the excluded volume and the hydration shell of the protein, these effects are negligible in our case when considering the error in the scattering intensity caused by the TFP molecules that were not present in the model. This was inspected by calculating intensities from the CaM-TFP crystal structure (1LIN). The radius of gyration R_g computed from 1LIN increases from 15.6 Å to 16.4 Å when the TFP density is removed. The removal of TFP molecules caused larger differences in the intensity at large s than the effects of the excluded volume and hydration shell, calculated by CRYSOL (Svergun et al., 1995). For the minimum conformation obtained by the procedure described above the χ^2 was also calculated with the program CRYSOL, which does take the hydration shell and the excluded volume into account (Eq. 1). This minimum corresponds to $\chi^2 = 2.4$. In the program CRYSOL, the excluded volume is represented using a two-dimensional en-

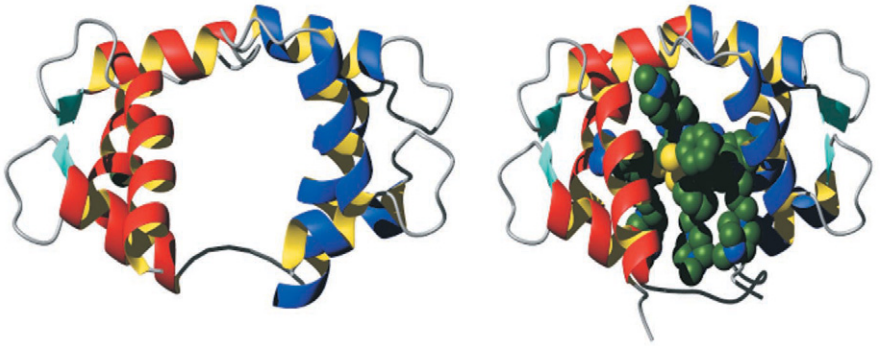

FIGURE 4 Model of calmodulin in complex with trifluoperazine (TFP) obtained by the combining NMR and SAXS data (*left*). The orientations of the N- and C-domains were determined from NMR measurements in an aqueous dilute liquid crystal and the most optimal mutual position of the domains was derived from SAXS data. Because no explicit information was acquired from the TFP molecules, they are not shown. For comparison the crystal structure of the complex (Vandonselaar et al., 1994) is shown (*right*). This figure was prepared by MOLMOL (Koradi et al., 1996).

velope function that may not adequately take into account the cavity between the domains of the model compared with a dummy atom representation for the excluded volume.

Comparison to the CaM-TFP crystal structure (1LIN) reveals that the model based on the SAXS and NMR data has closely similar relative domain orientations and distance between the domains (Fig. 4). When the 1LIN structure and our best solution are superimposed on their C^{α}-traces of residues 4–74 and 86–147 the RMSD is 2.4 Å. The distance between the centers of domains in the model is ~2 Å larger than in the crystal structure, almost entirely along the long axis of the shape tensor. Although this may be a genuine difference between the solution and crystal structures, other factors, most importantly the lack of TFP molecules from our model, contribute to the discrepancy. The TFP molecules were not included, because we did not want to define their positions a priori. The TFP molecules in 1LIN account for ~10% of the mass of the complex, meaning that the model is some 20% deficient in the scattering power at $I(0)$. The approximate positions of TFP molecules in the model were searched by placing them, one at a time, at Cartesian grid nodes of 1 Å spacing in x, y, and z, with three angles α, β, and γ stepped in 60° at each node. No van der Waals radii restrictions were applied. Minimum χ^2 values indicated that the first and second TFP molecules were localized in the central part of the model. For the third and fourth TFP molecule the fit improved but almost with no spatial information. As an alternative, we included an artificial spherical scatterer in the model between the domains to account for the scattering power of the TFP molecules. This improved the fit by ~15%. R_g decreased to 17.5 Å, but most improvements to the fit were at higher s values.

A minor contribution to χ^2 came from the few N-terminal residues of CaM that according to NMR data (Barbato et al., 1992) and nonexistent electron density (Meador et al., 1992) are not structured and therefore not included in the model. In our case where the lack of TFP molecules from the model accounts for most of the error there is also a small contribution from the hydration shell. It has been shown by comparison of SAXS and SANS data that neglecting the hydration shell will lead to a systematic error in R_g (Svergun et al., 1998), resulting in SAXS data producing a larger apparent structure by 1–2 Å. The CaM-TFP system therefore is a considerable challenge to the method, yet despite the incompleteness of the description of its components, the model is highly similar to the crystal structure (1LIN) (Fig. 4).

DISCUSSION

The ability to record NMR data to complement SAS data for larger proteins and their complexes has recently been developed through the exploitation of relaxation interference between dipole-dipole and chemical shift anisotropy interactions of the amide nuclei (TROSY) (Pervushin et al., 1997; Salzmann et al., 1998). The TROSY method is applicable to a large number of NMR experiments including the measurement of residual dipolar couplings from weakly aligned systems (Permi and Annila, 2000; Permi et al., 2000). Perdeuteration, a further means of NMR sensitivity enhancement for large complexes that can be domain specific or introduced segmentally within a protein using inteins (Yamazaki et al., 1998), limits the traditional short-range distance data that are obtainable, but assists the recording of residual dipolar couplings. Additionally, perdeuteration will serve to produce contrast for neutron scattering experiments. High contrast between the constituents of a complex coupled with high angular definition will further improve the possibilities to build high quality models from known subunits by SAS and NMR. Importantly for large systems, our method does not require complete assignment, but a few tens of unambiguous residual dipolar couplings will suffice (Clore, 2000). In this way structures of significantly larger protein complexes in solution can be studied than have been accomplished so far. In particular, homodimers or homo-oligomers are especially amenable to such model building owing to the symmetry constraints.

The precision with which orientations of domains can be defined depends on the number of residual dipolar couplings and their precision measured in nonredundant directions and on the structural agreement between the couplings and the individual high-resolution domains structures determined by x-ray crystallography or NMR spectroscopy. A

dense sampling of directions will also assist the detection of local structural changes. A portion of the couplings may also be affected by dynamics within each domain or conformational exchange within a domain (Tolman et al., 2001; Meiler et al., 2001). Methods to cross-validate the data (Skrynnikov and Kay, 2000) and ways to refine the models (Chou et al., 2001) have been developed. Asymmetry within the constituents of the complex will improve the precision, because fewer degrees of freedom remain ambiguous from the SAXS measurements. The completeness of the model will also determine the precision, but as illustrated above, considerable incompleteness can be tolerated.

This study of ligand-induced globularization of CaM illustrates the principle of constructing overall solution structure models from high-resolution coordinates of domains or subunits on the basis of NMR data from weakly aligned systems and small-angle scattering data. From the small-angle scattering perspective, NMR residual dipolar coupling data serve to reduce angular degrees of freedom. Alternatively, this could also be achieved using anisotropy in chemical shielding (CSA) to give the orientation with respect to the molecular alignment frame (Sanders et al., 1994; Wu et al., 2001). From the NMR point of view, the SAS data serve to reduce the translational degrees of freedom. This combination of methods circumvents difficulties in the observation and assignment of short-range (<5 Å) distance restraints that limit current applications of residual dipolar couplings to rigid-body dynamics assembly of complexes (Clore, 2000). We anticipate that the demand to construct models of larger complexes will increase rapidly as the protein data bank grows in its structural diversity.

We are indebted to Andrea Hounslow and Clare Treritt for advice and assistance.

This work was supported by the Academy of Finland and Technology Agent of Finland (TEKES).

REFERENCES

Al-Hashimi, H. M., H. Valafar, M. Terrell, E. R. Zartler, M. K. Eidsness, and J. H. Prestegard. 2000. Variation of molecular alignment as a means of resolving orientational ambiguities in protein structures from dipolar couplings. *J. Magn. Reson.* 143:402–406.

Barbato, G., M. Ikura, L. E. Kay, R. W. Pastor, and A. Bax. 1992. Backbone dynamics of calmodulin studied by 15N relaxation using inverse detected two-dimensional NMR spectroscopy: the central helix is flexible. *Biochemistry.* 31:5269–5278.

Bastiaan, E. W., C. MacLean, P. C. M. van Zijl, and A. A. Bothner-By. 1987. High resolution NMR of liquids and gases: effects of magnetic-field-induced molecular alignment. *Annu. Rep. NMR Spectrosc.* 9:35–77.

Bax, A., G. Kontaxis, and N. Tjandra. 2001. Dipolar couplings in macromolecular structure determination. *Methods Enzymol.* 339:127–174.

Biekofsky, R. R., F. W. Muskett, J. M. Schmidt, S. R. Martin, J. P. Browne, P. M. Bayley, and J. Feeney. 1999. NMR approaches for monitoring domain orientations in calcium-binding proteins in solution using partial replacement of Ca^{2+} by Tb^{3+}. *FEBS Lett.* 460:519–526.

Chacon, P., F. Moran, J. F. Diaz, E. Pantos, and J. M. Andreu. 1998. Low-resolution structures of proteins in solution retrieved from x-ray scattering with a genetic algorithm. *Biophys. J.* 74:2760–2775.

Chattopadhyaya, R., W. E. Meador, A. R. Means, and F. A. Quiocho. 1992. Calmodulin structure refined at 1.7 Å resolution. *J. Mol. Biol.* 228: 1177–1192.

Chou, J. J., S. Li, C. B. Klee, and A. Bax. 2001. Solution structure of Ca(2+)-calmodulin reveals flexible hand-like properties of its domains. *Nat. Struct. Biol.* 8:990–997.

Clore, G. M. 2000. Accurate and rapid docking of protein-protein complexes on the basis of intermolecular nuclear Overhauser enhancement data and dipolar couplings by rigid body minimization. *Proc. Natl. Acad. Sci. U.S.A.* 97:9021–9025.

Clore, G. M., and A. M. Gronenborn. 1998. NMR structure determination of proteins and protein complexes larger than 20 kDa. *Curr. Opin. Chem. Biol.* 2:564–570.

Clore, G. M., A. M. Gronenborn, and A. Bax. 1998. A robust method for determining the magnitude of the fully asymmetric alignment tensor of oriented macromolecules in the absence of structural information. *J. Magn. Reson.* 133:216–221.

Cook, W. J., L. J. Walter, and M. R. Walter. 1994. Drug binding by calmodulin: crystal structure of a calmodulin-trifluoperazine complex. *Biochemistry.* 33:15259–15265.

Cordier, F., A. J. Dingley, and S. Grzesiek. 1999. A doublet-separated sensitivity-enhanced HSQC for the determination of scalar and dipolar one-bond J-couplings. *J. Biomol. NMR.* 13:175–180.

Craven, C. J., B. Whitehead, S. K. Jones, E. Thulin, G. M. Blackburn, and J. P. Waltho. 1996. Complexes formed between calmodulin and the antagonists J-8 and TFP in solution. *Biochemistry.* 35:10287–10299.

Doniach, S. 2001. Changes in biomolecular conformation seen by small angle x-ray scattering. *Chem. Rev.* 101:1763–1778.

Feigin, L. A., and D. I. Svergun. 1987. Structure Analysis by Small-Angle X-Ray and Neutron Scattering. Plenum Press, New York.

Glatter, O., and O. Kratky. 1982. Small Angle X-Ray Scattering. Academic Press, New York.

Hansen, M. R., L. Mueller, and A. Pardi. 1998. Tunable alignment of macromolecules by filamentous phage yields dipolar coupling interactions. *Nat. Struct. Biol.* 5:1065–1074.

Heidorn, D. B., P. A. Seeger, S. E. Rokop, D. K. Blumenthal, A. R. Means, H. Crespi, and J. Trewhella. 1989. Changes in the structure of calmodulin induced by a peptide based on the calmodulin-binding domain of myosin light chain kinase. *Biochemistry.* 28:6757–6764.

Heidorn, D. B., and J. Trewhella. 1988. Comparison of the crystal and solution structures of calmodulin and troponin C. *Biochemistry.* 27: 909–915.

Ikura, M., G. Barbato, C. B. Kleem, and A. Bax. 1992b. Solution structure of calmodulin and its complex with a myosin light chain kinase fragment. *Cell Calcium.* 13:391–400.

Ikura, M., G. M. Clore, A. M. Gronenborn, G. Zhu, C. B. Klee, and A. Bax. 1992a. Solution structure of a calmodulin-target peptide complex by multidimensional NMR. *Science.* 256:632–638.

Koch, M. H. J., and H. B. Stuhrmann. 1979. Neutron scattering studies of ribosomes. *Methods Enzymol.* 59:670–706.

Koradi, R., M. Billeter, and K. Wüthrich. 1996. MOLMOL: a program for display and analysis of macromolecular structures. *J. Mol. Graph.* 14: 51–55.

Losonczi, J. A., M. Andrec, M. W. Fischer, and J. H. Prestegard. 1999. Order matrix analysis of residual dipolar couplings using singular value decomposition. *J. Magn. Reson.* 138:334–342.

Matsushima, N., N. Hayashi, Y. Jinbo, and Y. Izumi. 2000. Ca^{2+}-bound calmodulin forms a compact globular structure on binding four trifluoperazine molecules in solution. *Biochem. J.* 347:211–215.

Meador, W. E., A. R. Means, and F. A. Quiocho. 1992. Target enzyme recognition by calmodulin: 2.4 Å structure of a calmodulin-peptide complex. *Science.* 257:1251–1255.

Meiler, J., J. J. Prompers, W. Peti, C. Griesinger, and R. Bruschweiler. 2001. Model-free approach to the dynamic interpretation of residual

dipolar couplings in globular proteins. *J. Am. Chem. Soc.* 123: 6098–60107.

Müller, J. J., G. Damaschun, and H. Schrauber. 1990. The highly resolved excess electron distance distribution of biopolymers in solution: calculation from intermediate-angle x-ray scattering and interpretation. *J. Appl. Crystallogr.* 23:26–34.

Osawa, M., M. B. Swindells, J. Tanikawa, T. Tanaka, T. Mase, T. Furuya, and M. Ikura. 1998. Solution structure of calmodulin-W-7 complex: the basis of diversity in molecular recognition. *J. Mol. Biol.* 276:165–176.

Osawa, M., H. Tokumitsu, M. B. Swindells, H. Kurihara, M. Orita, T. Shibanuma, T. Furuya, and M. Ikura. 1999. A novel target recognition revealed by calmodulin in complex with Ca^{2+}-calmodulin-dependent kinase kinase. *Nat. Struct. Biol.* 6:819–824.

Ottiger, M., and A. Bax. 1999. Bicelle-based liquid crystals for NMR-measurement of dipolar couplings at acidic and basic pH values. *J. Biomol. NMR.* 13:187–191.

Ottiger, M., F. Delaglio, and A. Bax. 1998. Measurement of J and dipolar couplings from simplified two-dimensional NMR spectra. *J. Magn. Reson.* 131:373–378.

Permi, P., and A. Annila. 2000. Transverse relaxation optimised spectroscopy for measurement of residual dipolar couplings from two-dimensional [^{15}N,^{1}H] correlation spectra. *J. Biomol. NMR.* 16:221–227.

Permi, P., P. R. Rosewear, and A. Annila. 2000. A Set of HNCO-TROSY based experiments for measurement of scalar and dipolar couplings. *J. Biomol. NMR.* 17:43–54.

Pervushin, K., R. Riek, G. Wider, and K. Wüthrich. 1997. Attenuated T2 relaxation by mutual cancellation of dipole-dipole coupling and chemical shift anisotropy indicates an avenue to NMR structures of very large biological macromolecules in solution. *Proc. Natl. Acad. Sci. U.S.A.* 94:12366–12371.

Salzmann, M., K. Pervushin, G. Wider, H. Senn, and K. Wüthrich. 1998. TROSY in triple-resonance experiments: new perspectives for sequential NMR assignment of large proteins. *Proc. Natl. Acad. Sci. U.S.A.* 95:13585–13590.

Sanders, C. R., B. J. Hare, K. P. Howard, and J. H. Prestegard. 1994. Magnetically-oriented phospholipid micelles as a tool for the study of membrane-associated molecules. *Prog. Nuclear Magn. Reson. Spectrosc.* 26:421–444.

Shao, I., and D. Tu. 1995. The Jacknife and Bootstrap. Springer-Verlag, New York.

Skrynnikov, N. R., and L. E. Kay. 2000. Assessment of molecular structure using frame-independent orientational restraints derived from residual dipolar couplings. *J. Biomol. NMR.* 18:239–252.

Stuhrmann, H. B. 1970. Ein neues Verfahren zur Bestimmung der Oberflächenform und der inneren Struktur von gelösten globulären Proteinen aus Röntgenkleinwinkelmessungen. *Z. Physik. Chem. Neue Folge.* 72: 177–198.

Svergun, D. I. 1992. Determination of the regularization parameter in indirect-transform methods using perceptual criteria. *J. Appl. Crystallogr.* 25:495–503.

Svergun, D. I. 1999. Restoring low resolution structure of biological macromolecules from solution scattering using simulated annealing. *Biophys. J.* 76:2879–2886.

Svergun, D. I., C. Barberato, and M. H. J. Koch. 1995. CRYSOL: a program to evaluate x-ray solution scattering of biological macromolecules from atomic coordinates. *J. Appl. Crystallogr.* 28:768–773.

Svergun, D. I., M. V. Petoukhov, and M. H. Koch. 2001. Determination of domain structure of proteins from x-ray solution scattering. *Biophys. J.* 80:2946–2953.

Svergun, D. I., S. Richard, M. H. Koch, Z. Sayers, S. Kuprin, and G. Zaccai. 1998. Protein hydration in solution: experimental observation by x-ray and neutron scattering. *Proc. Natl. Acad. Sci. U.S.A.* 95: 2267–2272.

Tjandra, N., and A. Bax. 1997. Direct measurement of distances and angles in biomolecules by NMR in a dilute liquid crystalline medium. *Science.* 278:1111–1114.

Tolman, J. R., J. M. Flanagan, M. A. Kennedy, and J. H. Prestegard. 1997. NMR evidence for slow collective motions in cyanometmyoglobin. *Nat. Struct. Biol.* 4:292–297.

Tolman, J. R., H. M. Al-Hashimi, L. E. Kay, and J. H. Prestegard. 2001. Structural and dynamic analysis of residual dipolar coupling data for proteins. *J. Am. Chem. Soc.* 123:1416–1424.

Trewhella, J. 1997. Insights into biomolecular function from small-angle scattering. *Curr. Opin. Struct. Biol.* 7:702–708.

Vandonselaar, M., R. A. Hickie, J. W. Quail, and L. T. Delbaere. 1994. Trifluoperazine-induced conformational change in Ca^{2+}-calmodulin. *Nat. Struct. Biol.* 1:795–801.

Wu, Z., N. Tjandra, and A. Bax. 2001. ^{31}P chemical shift anisotropy as an aid in determining nucleic acid structure in liquid crystals. *J. Am. Chem. Soc.* 123:3617–3618.

Yamazaki, T., T. Otomo, N. Oda, Y. Kyogoku, K. Uegaki, N. Ito, Y. Ishino, and H. Nakamura. 1998. Segmental isotope labeling for protein NMR using peptide splicing. *J. Am. Chem. Soc.* 120:5591–5592.